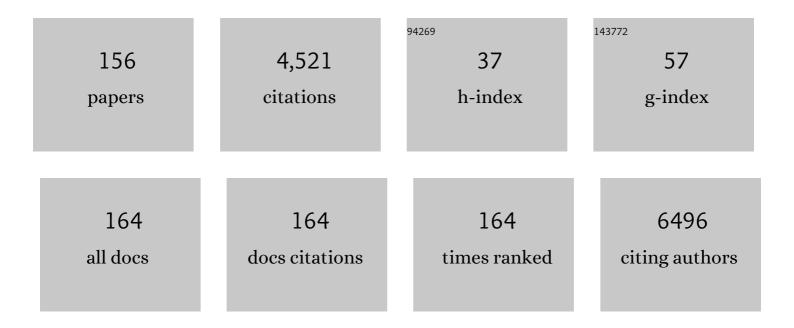
## Haitao Wang

List of Publications by Year in descending order

Source: https://exaly.com/author-pdf/914594/publications.pdf Version: 2024-02-01



ΗΛΙΤΛΟ ΜΛΝΟ

#	Article	IF	CITATIONS
1	FOXO Signaling Pathways as Therapeutic Targets in Cancer. International Journal of Biological Sciences, 2017, 13, 815-827.	2.6	338
2	cAMP Response Element-Binding Protein (CREB): A Possible Signaling Molecule Link in the Pathophysiology of Schizophrenia. Frontiers in Molecular Neuroscience, 2018, 11, 255.	1.4	250
3	Core-shell iron oxide-layered double hydroxide: High electrochemical sensing performance of H2O2 biomarker in live cancer cells with plasma therapeutics. Biosensors and Bioelectronics, 2017, 97, 352-359.	5.3	135
4	Superlattice stacking by hybridizing layered double hydroxide nanosheets with layers of reduced graphene oxide for electrochemical simultaneous determination of dopamine, uric acid and ascorbic acid. Mikrochimica Acta, 2019, 186, 61.	2.5	133
5	Hollow Nitrogen-Doped Carbon Spheres with Fe <sub>3</sub> O <sub>4</sub> Nanoparticles Encapsulated as a Highly Active Oxygen-Reduction Catalyst. ACS Applied Materials & Interfaces, 2017, 9, 10610-10617.	4.0	128
6	The possible role of the Akt signaling pathway in schizophrenia. Brain Research, 2012, 1470, 145-158.	1.1	106
7	Liquid biopsy tracking during sequential chemo-radiotherapy identifies distinct prognostic phenotypes in nasopharyngeal carcinoma. Nature Communications, 2019, 10, 3941.	5.8	98
8	FFPM, a PDE4 inhibitor, reverses learning and memory deficits in APP/PS1 transgenic mice via cAMP/PKA/CREB signaling and anti-inflammatory effects. Neuropharmacology, 2017, 116, 260-269.	2.0	96
9	Candida albicans gains azole resistance by altering sphingolipid composition. Nature Communications, 2018, 9, 4495.	5.8	89
10	Uniform Fe <sub>3</sub> O <sub>4</sub> /Nitrogen-Doped Mesoporous Carbon Spheres Derived from Ferric Citrate-Bonded Melamine Resin as an Efficient Synergistic Catalyst for Oxygen Reduction. ACS Applied Materials & Interfaces, 2017, 9, 335-344.	4.0	82
11	Drug screening of cancer cell lines and human primary tumors using droplet microfluidics. Scientific Reports, 2017, 7, 9109.	1.6	69
12	Inhibition of PDE4 protects neurons against oxygen-glucose deprivation-induced endoplasmic reticulum stress through activation of the Nrf-2/HO-1 pathway. Redox Biology, 2020, 28, 101342.	3.9	68
13	Protective mechanism of artemisinin on rat bone marrow-derived mesenchymal stem cells against apoptosis induced by hydrogen peroxide via activation of c-Raf-Erk1/2-p90rsk-CREB pathway. Stem Cell Research and Therapy, 2019, 10, 312.	2.4	65
14	The Nerve Growth Factor Signaling and Its Potential as Therapeutic Target for Glaucoma. BioMed Research International, 2014, 2014, 1-10.	0.9	64
15	Use of low-field-NMR and MRI to characterize water mobility and distribution in pacific oyster ( <i>Crassostrea gigas</i> ) during drying process. Drying Technology, 2018, 36, 630-636.	1.7	63
16	Artemisinin conferred ERK mediated neuroprotection to PC12 cells and cortical neurons exposed to sodium nitroprusside-induced oxidative insult. Free Radical Biology and Medicine, 2016, 97, 158-167.	1.3	60
17	RNA Interference-Mediated Knockdown of Long-Form Phosphodiesterase-4D (PDE4D) Enzyme Reverses Amyloid-β42-Induced Memory Deficits in Mice. Journal of Alzheimer's Disease, 2013, 38, 269-280.	1.2	59
18	UCSCXenaShiny: an R/CRAN package for interactive analysis of UCSC Xena data. Bioinformatics, 2022, 38, 527-529.	1.8	59

#	Article	IF	CITATIONS
19	Self-assembly of highly luminescent bi-1,3,4-oxadiazole derivatives through electron donor–acceptor interactions in three-dimensional crystals, two-dimensional layers and mesophases. Journal of Materials Chemistry, 2008, 18, 3954.	6.7	56
20	Cerebrovascular Safety of Sulfonylureas: The Role of KATP Channels in Neuroprotection and the Risk of Stroke in Patients With Type 2 Diabetes. Diabetes, 2016, 65, 2795-2809.	0.3	56
21	Cisplatin prevents breast cancer metastasis through blocking early EMT and retards cancer growth together with paclitaxel. Theranostics, 2021, 11, 2442-2459.	4.6	56
22	The role of Akt/FoxO3a in the protective effect of venlafaxine against corticosterone-induced cell death in PC12 cells. Psychopharmacology, 2013, 228, 129-141.	1.5	55
23	Inhibition of phosphodiesterase 4 by FCPR16 protects SH-SY5Y cells against MPP+-induced decline of mitochondrial membrane potential and oxidative stress. Redox Biology, 2018, 16, 47-58.	3.9	55
24	In situ polymerization and characterization of polyamide-6/silica nanocomposites derived from water glass. Polymer International, 2004, 53, 1153-1160.	1.6	53
25	Forkhead box O transcription factors as possible mediators in the development of major depression. Neuropharmacology, 2015, 99, 527-537.	2.0	50
26	Real-time tracking of hydrogen peroxide secreted by live cells using MnO2 nanoparticles intercalated layered doubled hydroxide nanohybrids. Analytica Chimica Acta, 2015, 898, 34-41.	2.6	50
27	Epigenetic targeting drugs potentiate chemotherapeutic effects in solid tumor therapy. Scientific Reports, 2017, 7, 4035.	1.6	49
28	Molecular landscape and subtype-specific therapeutic response of nasopharyngeal carcinoma revealed by integrative pharmacogenomics. Nature Communications, 2021, 12, 3046.	5.8	48
29	Roflumilast prevents ischemic stroke-induced neuronal damage by restricting GSK3β-mediated oxidative stress and IRE1α/TRAF2/JNK pathway. Free Radical Biology and Medicine, 2021, 163, 281-296.	1.3	47
30	Involvement of PI3K/Akt/FoxO3a and PKA/CREB Signaling Pathways in the Protective Effect of Fluoxetine Against Corticosterone-Induced Cytotoxicity in PC12 Cells. Journal of Molecular Neuroscience, 2016, 59, 567-578.	1.1	46
31	Transient receptor potential melastatin 2 channels (TRPM2) mediate neonatal hypoxic-ischemic brain injury in mice. Experimental Neurology, 2017, 296, 32-40.	2.0	46
32	Hydrazide-based organogels and liquid crystals with columnar order. New Journal of Chemistry, 2007, 31, 401.	1.4	45
33	Molecular Basis of Substrate Specific Acetylation by N-Terminal Acetyltransferase NatB. Structure, 2017, 25, 641-649.e3.	1.6	44
34	Ammonium tetrathiomolybdate treatment targets the copper transporter ATP7A and enhances sensitivity of breast cancer to cisplatin. Oncotarget, 2016, 7, 84439-84452.	0.8	42
35	FCPR03, a novel phosphodiesterase 4 inhibitor, alleviates cerebral ischemia/reperfusion injury through activation of the AKT/GSK3î²/ î²-catenin signaling pathway. Biochemical Pharmacology, 2019, 163, 234-249.	2.0	42
36	IGF-1 Signaling via the PI3K/Akt Pathway Confers Neuroprotection in Human Retinal Pigment Epithelial Cells Exposed to Sodium Nitroprusside Insult. Journal of Molecular Neuroscience, 2015, 55, 931-940.	1.1	41

#	Article	IF	CITATIONS
37	Tideglusib, a chemical inhibitor of CSK3β, attenuates hypoxic-ischemic brain injury in neonatal mice. Biochimica Et Biophysica Acta - General Subjects, 2016, 1860, 2076-2085.	1.1	40
38	BRCA1 Deficiency Impairs Mitophagy and Promotes Inflammasome Activation and Mammary Tumor Metastasis. Advanced Science, 2020, 7, 1903616.	5.6	39
39	Comparison of radiomics tools for image analyses and clinical prediction in nasopharyngeal carcinoma. British Journal of Radiology, 2019, 92, 20190271.	1.0	38
40	Roflupram, a Phosphodiesterase 4 Inhibitior, Suppresses Inflammasome Activation through Autophagy in Microglial Cells. ACS Chemical Neuroscience, 2017, 8, 2381-2392.	1.7	36
41	Inhibition of phosphodiesterase-4 suppresses HMGB1/RAGE signaling pathway and NLRP3 inflammasome activation in mice exposed to chronic unpredictable mild stress. Brain, Behavior, and Immunity, 2021, 92, 67-77.	2.0	36
42	Transcriptome Sequencing of Gracilariopsis lemaneiformis to Analyze the Genes Related to Optically Active Phycoerythrin Synthesis. PLoS ONE, 2017, 12, e0170855.	1.1	35
43	Inhibition of PDE4 by FCPR16 induces AMPK-dependent autophagy and confers neuroprotection in SH-SY5Y cells and neurons exposed to MPP+-induced oxidative insult. Free Radical Biology and Medicine, 2019, 135, 87-101.	1.3	34
44	Roflupram exerts neuroprotection via activation of CREB/PGCâ€1α signalling in experimental models of Parkinson's disease. British Journal of Pharmacology, 2020, 177, 2333-2350.	2.7	34
45	Somatostatin receptor 2 expression in nasopharyngeal cancer is induced by Epstein Barr virus infection: impact on prognosis, imaging and therapy. Nature Communications, 2021, 12, 117.	5.8	34
46	<scp>GSK</scp> â€3β inhibitor <scp>TDZD</scp> â€8 reduces neonatal hypoxicâ€ischemic brain injury in mice. CNS Neuroscience and Therapeutics, 2017, 23, 405-415.	1.9	33
47	LncRNA DINOR is a virulence factor and global regulator of stress responses in Candida auris. Nature Microbiology, 2021, 6, 842-851.	5.9	31
48	Dysbindin-1 Involvement in the Etiology of Schizophrenia. International Journal of Molecular Sciences, 2017, 18, 2044.	1.8	30
49	Protein Phosphatase Pph3 and Its Regulatory Subunit Psy2 Regulate Rad53 Dephosphorylation and Cell Morphogenesis during Recovery from DNA Damage in Candida albicans. Eukaryotic Cell, 2011, 10, 1565-1573.	3.4	29
50	Artemisinin Protects Retinal Neuronal Cells against Oxidative Stress and Restores Rat Retinal Physiological Function from Light Exposed Damage. ACS Chemical Neuroscience, 2017, 8, 1713-1723.	1.7	29
51	Berberine Protects Human Retinal Pigment Epithelial Cells from Hydrogen Peroxide-Induced Oxidative Damage through Activation of AMPK. International Journal of Molecular Sciences, 2018, 19, 1736.	1.8	29
52	Forkhead family transcription factor FoxO and neural differentiation. Neurogenetics, 2012, 13, 105-113.	0.7	28
53	FoxO3a Negatively Regulates Nerve Growth Factor-Induced Neuronal Differentiation Through Inhibiting the Expression of Neurochondrin in PC12 Cells. Molecular Neurobiology, 2013, 47, 24-36.	1.9	28
54	The phosphodiesterase-4 inhibitor, FCPR16, attenuates ischemia-reperfusion injury in rats subjected to middle cerebral artery occlusion and reperfusion. Brain Research Bulletin, 2018, 137, 98-106.	1.4	28

#	Article	IF	CITATIONS
55	Targeting phosphodiesterase 4 as a potential therapeutic strategy for enhancing neuroplasticity following ischemic stroke. International Journal of Biological Sciences, 2018, 14, 1745-1754.	2.6	28
56	Roflumilast reverses polymicrobial sepsis-induced liver damage by inhibiting inflammation in mice. Laboratory Investigation, 2017, 97, 1008-1019.	1.7	27
57	Lithium ions attenuate serum-deprivation-induced apoptosis in PC12 cells through regulation of the Akt/FoxO1 signaling pathways. Psychopharmacology, 2016, 233, 785-794.	1.5	26
58	Electrospun Polyurethane/Zeolitic Imidazolate Framework Nanofibrous Membrane with Superior Stability for Filtering Performance. ACS Applied Polymer Materials, 2021, 3, 710-719.	2.0	26
59	Multiâ€omics consensus ensemble refines the classification of muscleâ€invasive bladder cancer with stratified prognosis, tumour microenvironment and distinct sensitivity to frontline therapies. Clinical and Translational Medicine, 2021, 11, e601.	1.7	25
60	Light-driven fluorescence enhancement and self-assembled structural evolution of an azobenzene derivative. Journal of Materials Chemistry C, 2014, 2, 9866-9873.	2.7	24
61	New "haploid biofilm model―unravels IRA2 as a novel regulator of Candida albicans biofilm formation. Scientific Reports, 2015, 5, 12433.	1.6	24
62	Microglia-Synapse Pathways: Promising Therapeutic Strategy for Alzheimer's Disease. BioMed Research International, 2017, 2017, 1-11.	0.9	22
63	The involvement of DARPP-32 in the pathophysiology of schizophrenia. Oncotarget, 2017, 8, 53791-53803.	0.8	22
64	FCPR16, a novel phosphodiesterase 4 inhibitor, produces an antidepressant-like effect in mice exposed to chronic unpredictable mild stress. Progress in Neuro-Psychopharmacology and Biological Psychiatry, 2019, 90, 62-75.	2.5	22
65	Pph3 Dephosphorylation of Rad53 Is Required for Cell Recovery from MMS-Induced DNA Damage in Candida albicans. PLoS ONE, 2012, 7, e37246.	1.1	22
66	Insulin-like growth factor-1 induces the phosphorylation of PRAS40 via the PI3K/Akt signaling pathway in PC12 cells. Neuroscience Letters, 2012, 516, 105-109.	1.0	21
67	Nerve growth factor protects retinal ganglion cells against injury induced by retinal ischemia–reperfusion in rats. Growth Factors, 2015, 33, 149-159.	0.5	21
68	Multistimuli-responsive organogels based on hydrazide and azobenzene derivatives. RSC Advances, 2017, 7, 218-223.	1.7	21
69	Multistimuli-Responsive Fluorescent Organogelator Based on Triphenylamine-Substituted Acylhydrazone Derivative. ACS Omega, 2020, 5, 5675-5683.	1.6	21
70	The mitochondrial protein Mcu1 plays important roles in carbon source utilization, filamentation, and virulence in Candida albicans. Fungal Genetics and Biology, 2015, 81, 150-159.	0.9	20
71	Insulinâ€like growth factorâ€1 activates PI3K/Akt signalling to protect human retinal pigment epithelial cells from amiodaroneâ€induced oxidative injury. British Journal of Pharmacology, 2018, 175, 125-139.	2.7	20
72	Tanshinone IIA Attenuates Insulin Like Growth Factor 1 -Induced Cell Proliferation in PC12 Cells through the PI3K/Akt and MEK/ERK Pathways. International Journal of Molecular Sciences, 2018, 19, 2719.	1.8	20

#	Article	IF	CITATIONS
73	Liquid crystalline behaviour of benzoic acid derivatives containing alkoxyazobenzene. Liquid Crystals, 2007, 34, 659-665.	0.9	19
74	Hederagenin Protects PC12 Cells Against Corticosterone-Induced Injury by the Activation of the PI3K/AKT Pathway. Frontiers in Pharmacology, 2021, 12, 712876.	1.6	19
75	Nonâ€ <b>s</b> ymmetric liquid crystal dimers containing the 4â€ <b>n</b> itrobenzohydrazide group: synthesis and mesomorphic behaviour. Liquid Crystals, 2008, 35, 793-798.	0.9	18
76	The synthesis and mesomorphic behaviour of tetracatenar and hexacatenar biâ€1,3,4â€oxadiazole derivatives. Liquid Crystals, 2009, 36, 7-12.	0.9	18
77	Organogels from unsymmetrical π-conjugated 1,3,4-oxadiazole derivatives. New Journal of Chemistry, 2013, 37, 1454.	1.4	18
78	Novel Mechanism Coupling Cyclic AMP-Protein Kinase A Signaling and Golgi Trafficking via Gyp1 Phosphorylation in Polarized Growth. Eukaryotic Cell, 2014, 13, 1548-1556.	3.4	18
79	Inhibition of Phosphodiesterase 4 by FCPR03 Alleviates Lipopolysaccharide-Induced Depressive-Like Behaviors in Mice: Involvement of p38 and JNK Signaling Pathways. International Journal of Molecular Sciences, 2018, 19, 513.	1.8	18
80	Inhibition of Phosphodiesterase 4 by FCPR03 Alleviates Chronic Unpredictable Mild Stress-Induced Depressive-Like Behaviors and Prevents Dendritic Spine Loss in Mice Hippocampi. International Journal of Neuropsychopharmacology, 2019, 22, 143-156.	1.0	18
81	Anti-NMDAR encephalitis induced in mice by active immunization with a peptide from the amino-terminal domain of the GluN1 subunit. Journal of Neuroinflammation, 2021, 18, 53.	3.1	17
82	Helical ribbons tuned by alkoxy chains in achiral twin-tapered dihydrazide derivatives. New Journal of Chemistry, 2008, 32, 2023.	1.4	16
83	A new series of liquidâ€crystalline biâ€1,3,4â€oxadiazole derivatives: synthesis and mesomorphic behaviour. Liquid Crystals, 2008, 35, 389-394.	0.9	16
84	The synthesis and mesomorphic behaviour of tetracatenar di-hydrazine derivatives. Liquid Crystals, 2009, 36, 817-824.	0.9	16
85	Glutamate attenuates IGF-1 receptor tyrosine phosphorylation in mouse brain: Possible significance in ischemic brain damage. Neuroscience Research, 2012, 74, 290-297.	1.0	16
86	Control of self-assembly of twin-tapered dihydrazide derivative: mesophase and fluorescence-enhanced organogels. RSC Advances, 2013, 3, 12109.	1.7	16
87	Inhibition of PDE4 Attenuates TNF-α-Triggered Cell Death Through Suppressing NF-κB and JNK Activation in HT-22 Neuronal Cells. Cellular and Molecular Neurobiology, 2020, 40, 421-435.	1.7	16
88	Low molecular mass organogel from mesomorphic Nâ€(4â€hexyloxybenzoyl)â€N′â€(4′â€nitrobenzoyl)hyd Liquid Crystals, 2006, 33, 439-443.	razine. 0.9	15
89	Observation of intercalated smectic phases in symmetric liquid crystal dimers containing hydrazide groups. Liquid Crystals, 2006, 33, 445-450.	0.9	14
90	Gelation behaviour and gel properties of two-component organogels containing a photoresponsive gelator. New Journal of Chemistry, 2017, 41, 8614-8619.	1.4	14

#	Article	IF	CITATIONS
91	Roflupram, a novel phosphodiesterase 4 inhibitor, inhibits lipopolysaccharide-induced neuroinflammatory responses through activation of the AMPK/Sirt1 pathway. International Immunopharmacology, 2021, 90, 107176.	1.7	14
92	Genistein inhibits PDGF-stimulated proteoglycan synthesis in vascular smooth muscle without blocking PDGFβ receptor phosphorylation. Archives of Biochemistry and Biophysics, 2012, 525, 25-31.	1.4	13
93	Shp1, a regulator of protein phosphatase 1 Glc7, has important roles in cell morphogenesis, cell cycle progression and DNA damage response in Candida albicans. Fungal Genetics and Biology, 2012, 49, 433-442.	0.9	13
94	Regulation of <scp>Rfa2</scp> phosphorylation in response to genotoxic stress in <scp><i>C</i></scp> <i>andida albicans</i> . Molecular Microbiology, 2014, 94, 141-155.	1.2	13
95	CDK phosphorylates the polarisome scaffold Spa2 to maintain its localization at the site of cell growth. Molecular Microbiology, 2016, 101, 250-264.	1.2	13
96	Rfa2 is specifically dephosphorylated by Pph3 in <i>Candida albicans</i> . Biochemical Journal, 2013, 449, 673-681.	1.7	12
97	Platelet-derived growth factor-stimulated versican synthesis but not glycosaminoglycan elongation in vascular smooth muscle is mediated via Akt phosphorylation. Cellular Signalling, 2014, 26, 912-916.	1.7	12
98	IGF-1-Mediated Survival from Induced Death of Human Primary Cultured Retinal Pigment Epithelial Cells Is Mediated by an Akt-Dependent Signaling Pathway. Molecular Neurobiology, 2018, 55, 1915-1927.	1.9	12
99	PRDM3 attenuates pancreatitis and pancreatic tumorigenesis by regulating inflammatory response. Cell Death and Disease, 2020, 11, 187.	2.7	11
100	Genome-wide piggyBac transposon-based mutagenesis and quantitative insertion-site analysis in haploid Candida species. Nature Protocols, 2020, 15, 2705-2727.	5.5	10
101	Morphology and Wettability Tunable Organogel System Based on An 1,3,4-Oxadiazole Derivative. Soft Materials, 2014, 12, 396-402.	0.8	9
102	Elicitation of Jerusalem artichoke ( <i>Helianthus tuberosus</i> L.) cell suspension culture for enhancement of inulin production and altered degree of polymerisation. Journal of the Science of Food and Agriculture, 2017, 97, 88-94.	1.7	9
103	A mechano-responsive fluorescent xerogel based on an anthracene-substituted acylhydrazone derivative. New Journal of Chemistry, 2019, 43, 5214-5218.	1.4	9
104	Enhanced Protein Damage Clearance Induces Broad Drug Resistance in Multitype of Cancers Revealed by an Evolution Drugâ€Resistant Model and Genomeâ€Wide siRNA Screening. Advanced Science, 2020, 7, 2001914.	5.6	9
105	Development of a risk classification system combining TN-categories and circulating EBV DNA for non-metastatic NPC in 10,149 endemic cases. Therapeutic Advances in Medical Oncology, 2021, 13, 175883592110524.	1.4	9
106	Hydrazide-based non-symmetric liquid crystal dimers: synthesis and mesomorphic behavior. Journal of Physical Organic Chemistry, 2007, 20, 589-593.	0.9	8
107	Synthesis and liquid crystalline properties of hydrazide derivatives: hydrogen bonding, molecular dipole, and smectic structures. Liquid Crystals, 2008, 35, 333-338.	0.9	8
108	Anticlinic smectic phase formed by calamitic hydrazide derivatives with terminal hydroxyl group. Liquid Crystals, 2011, 38, 1227-1237.	0.9	8

#	Article	IF	CITATIONS
109	Liquid crystalline behaviour of hydrazide derivatives containing alkoxyazobenzene. Liquid Crystals, 2014, 41, 214-221.	0.9	8
110	Cloning and transcription analysis of the nitrate reductase gene from Haematococcus pluvialis. Biotechnology Letters, 2017, 39, 589-597.	1.1	8
111	Observation of Morphology and Structure Evolution during Gelation of a Bis(Anhydrazide) Derivative. Journal of Physical Chemistry B, 2017, 121, 8795-8801.	1.2	8
112	Changes in the Photosynthetic Pigment Contents and Transcription Levels of Phycoerythrin-Related Genes in Three Gracilariopsis lemaneiformis Strains Under Different Light Intensities. Journal of Ocean University of China, 2021, 20, 661-668.	0.6	8
113	Cullin3 deficiency shapes tumor microenvironment and promotes cholangiocarcinoma in liver-specific Smad4/Pten mutant mice. International Journal of Biological Sciences, 2021, 17, 4176-4191.	2.6	7
114	Roflupram attenuates α-synuclein-induced cytotoxicity and promotes the mitochondrial translocation of Parkin in SH-SY5Y cells overexpressing A53T mutant α-synuclein. Toxicology and Applied Pharmacology, 2022, 436, 115859.	1.3	7
115	C-Reactive Protein Induces Tau Hyperphosphorylation via GSK3β Signaling Pathway in SH-SY5Y Cells. Journal of Molecular Neuroscience, 2015, 56, 519-527.	1.1	6
116	Solvent-dependent gelation behaviour and liquid crystal properties of a bent-core dihydrazide derivative. New Journal of Chemistry, 2017, 41, 9482-9488.	1.4	6
117	Exploring the difference in xerogels and organogels through <i>in situ</i> observation. Royal Society Open Science, 2018, 5, 170492.	1.1	6
118	Multiple stimulus-responsive behavior of a triphenylamine-substituted acylhydrazone derivative. New Journal of Chemistry, 2021, 45, 2085-2089.	1.4	6
119	A Photoâ€Responsive Organogel Based on Pyreneâ€&ubstituted Acylhydrazone Derivative. Chinese Journal of Chemistry, 2017, 35, 1829-1834.	2.6	5
120	Sirt1 deficiency upregulates glutathione metabolism to prevent hepatocellular carcinoma initiation in mice. Oncogene, 2021, 40, 6023-6033.	2.6	5
121	H2O2 attenuates IGF-1R tyrosine phosphorylation and its survival signaling properties in neuronal cells via NR2B containing NMDA receptor. Oncotarget, 2017, 8, 65313-65328.	0.8	5
122	Multicolor fluorescence switching material induced by force and acid. Spectrochimica Acta - Part A: Molecular and Biomolecular Spectroscopy, 2022, 268, 120631.	2.0	5
123	Protective trend of anti-androgen therapy during the COVID-19 pandemic: A meta-analysis. Journal of Infection, 2022, 84, 834-872.	1.7	5
124	Transforming primary human hepatocytes into hepatocellular carcinoma with genetically defined factors. EMBO Reports, 2022, , e54275.	2.0	5
125	Liquid Crystalline Behaviours of the Complexes Based on 1,3,4â€Oxadiazole Derivative and Benzoic Acid. Chinese Journal of Chemistry, 2012, 30, 785-790.	2.6	4
126	Kinetic and Morphological Studies of Two Different Topological Structures Developed from <i>N, N</i> '-Bis (4-N-Alkylo-Xybenzoyl) Hydrazine (4D <sub>16</sub> ) Organogel. Soft Materials, 2014, 12, 230-236.	0.8	4

#	Article	IF	CITATIONS
127	Synthesis and mesomorphic behaviour of hexacatenar di-hydrazine derivatives. Liquid Crystals, 2014, 41, 1854-1861.	0.9	4
128	Effects of carbon nanomaterials on the aggregation of a bi-oxadiazole derivative (BOXD-T8) in DMF and its gel properties. New Journal of Chemistry, 2014, 38, 4823-4829.	1.4	4
129	Benzohydrazide Derivatives: Gelation and Application in Oil Spill Recovery. Chemical Research in Chinese Universities, 2019, 35, 874-878.	1.3	4
130	Stimuli-responsive behavior of naphthyl acylhydrazone derivative and its application in information security protection. Spectrochimica Acta - Part A: Molecular and Biomolecular Spectroscopy, 2020, 242, 118768.	2.0	4
131	Bionic research on spikes based on the tractive characteristics of ostrich foot toenail. Simulation, 2020, 96, 713-723.	1.1	4
132	Direct evidence for the effect of intermolecular hydrogen bonding on organogels. Chemical Research in Chinese Universities, 2014, 30, 821-824.	1.3	3
133	Role of Ppt1 in multiple stress responses in Candida albicans. Science Bulletin, 2014, 59, 4060-4068.	1.7	3
134	An NMR study on the gelation of N,N′-bis(4-N-alkylo-xybenzoyl) hydrazine (4Dn) in two aromatic solvents. New Journal of Chemistry, 2015, 39, 2711-2719.	1.4	3
135	The effect of molecular structure on the chiral random grain boundary phase. Liquid Crystals, 2018, 45, 1234-1241.	0.9	3
136	Cloning of the pcyA gene from Arthrospira platensis FACHB314 and its function on expression of a fluorescent phycocyanin in heterologous hosts. Journal of Applied Phycology, 2019, 31, 3665-3675.	1.5	3
137	FEM analysis in excellent cushion characteristic of ostrich (Struthio camelus) toe pads. PLoS ONE, 2019, 14, e0216141.	1.1	3
138	The metabolic footprint during adipocyte commitment highlights ceramide modulation as an adequate approach for obesity treatment. EBioMedicine, 2020, 51, 102605.	2.7	3
139	Glutamate Attenuates the Survival Property of IGFR through NR2B Containing N-Methyl-D-aspartate Receptors in Cortical Neurons. Oxidative Medicine and Cellular Longevity, 2020, 2020, 1-13.	1.9	3
140	High-Dimensional Characterization of the Systemic Immune Landscape Informs on Synergism Between Radiation Therapy and Immune Checkpoint Blockade. International Journal of Radiation Oncology Biology Physics, 2020, 108, 70-80.	0.4	3
141	BRCA1 Deficiency: BRCA1 Deficiency Impairs Mitophagy and Promotes Inflammasome Activation and Mammary Tumor Metastasis (Adv. Sci. 6/2020). Advanced Science, 2020, 7, 2070033.	5.6	3
142	Upregulation of amplified in breast cancer 1 contributes to pancreatic ductal adenocarcinoma progression and vulnerability to blockage of hedgehog activation. Theranostics, 2021, 11, 1672-1689.	4.6	3
143	Gel Ability and Fluorescence-Enhanced Emission of a New Bi-1,3,4-Oxadiazole Derivative. Soft Materials, 2013, 11, 261-271.	0.8	2
144	Gelation behavior and structure transition in mixtures of disc-shape dihydrazide derivative. Soft Materials, 2017, 15, 255-262.	0.8	2

#	ARTICLE	IF	CITATIONS
145	Force-, heat- and acid-induced fluorescent switching properties of an anthracene-based hydrazide derivative. Spectrochimica Acta - Part A: Molecular and Biomolecular Spectroscopy, 2021, 256, 119752.	2.0	2
146	Gelation behavior, anion response, and toxic dyes removal properties of a symmetrical dihydrazide derivative. Soft Materials, 2019, 17, 383-390.	0.8	1
147	Research on detection scheme of pebbles in fuel handling system pipelines in pebble-bed HTGR based on γ-ray measurement. Applied Radiation and Isotopes, 2021, 171, 109619.	0.7	1
148	Immune dysregulation underpins radioresistance in nasopharyngeal carcinoma (NPC) Journal of Global Oncology, 2019, 5, 52-52.	0.5	1
149	Assessment of chimeric antigen receptor T cytotoxicity by droplet microfluidics in vitro. Antibody Therapeutics, 2022, 5, 85-99.	1.2	1
150	Radio-Transcriptomic Phenotypes Predict Radioresistance in Nasopharyngeal Carcinoma. International Journal of Radiation Oncology Biology Physics, 2019, 105, E388-E389.	0.4	0
151	Phase transition behaviors of the self-assembled structures of a dihydrazide derivative. Soft Materials, 2020, 18, 67-73.	0.8	0
152	Cisplatin prevents breast cancer metastasis through blocking early EMT and retards cancer growth together with paclitaxel. FASEB Journal, 2021, 35, .	0.2	0
153	Abstract 2416: Upregulation of amplified in breast cancer 1 contributes to pancreatic ductal adenocarcinoma progression and vulnerability to blockage of hedgehog activation. , 2021, , .		0
154	A novel computational OMICS and non-OMICS approach for identifying true pathogenic risk variants for Asian prostate cancer Journal of Global Oncology, 2019, 5, 47-47.	0.5	0
155	Preliminary outcomes of a prospective observational study of combinatorial abiraterone acetate/enzalutamide (AA/Enz) and radical radiotherapy (RT) in nonmetastatic node-positive (N+MO) prostate cancer (PCa) Journal of Clinical Oncology, 2020, 38, 227-227.	0.8	0
156	2670 Distinct phenotypes of locoregionally advanced (LA-NPC) harbor disparate survival outcomes and are associated with germline variants. Annals of Oncology, 2020, 31, S1347-S1348.	0.6	0